



**HAL**  
open science

## Second Harmonic and Hyper-Rayleigh Generation of (111) silicon wafer

Laetitia Dalstein, Marc Tondusson, Jérôme Degert, Eric Freysz

► **To cite this version:**

Laetitia Dalstein, Marc Tondusson, Jérôme Degert, Eric Freysz. Second Harmonic and Hyper-Rayleigh Generation of (111) silicon wafer. 48th International Conference on Infrared, Millimeter and Terahertz Waves (IRMMW-THz 2023), IRMMW-THz Society, Sep 2023, Montréal Québec, Canada. hal-04185837

**HAL Id: hal-04185837**

**<https://hal.science/hal-04185837>**

Submitted on 23 Aug 2023

**HAL** is a multi-disciplinary open access archive for the deposit and dissemination of scientific research documents, whether they are published or not. The documents may come from teaching and research institutions in France or abroad, or from public or private research centers.

L'archive ouverte pluridisciplinaire **HAL**, est destinée au dépôt et à la diffusion de documents scientifiques de niveau recherche, publiés ou non, émanant des établissements d'enseignement et de recherche français ou étrangers, des laboratoires publics ou privés.

# Second Harmonic and Hyper-Rayleigh Generation of (111) silicon wafer

L. Dalstein<sup>1</sup>, M. Tondusson<sup>1</sup>, J. Degert<sup>1</sup> and E. Freysz<sup>1</sup>  
<sup>1</sup>Univ. Bordeaux, CNRS, LOMA UMR 5798, 33405 Talence, FRANCE

**Ultrafast time-resolved THz-induced SHG, also named hyper-Rayleigh generation, is performed at the surface of a (111) silicon wafer upon its excitation by a 50 fs IR optical pulse. The evolution of the SHG spectrum is recorded delaying in time the optical pulse with respect to the THz pulse. Upon excitation, we record a broad Stokes and anti-Stokes bands centered around the Si lattice phonon at  $\sim 610 \text{ cm}^{-1}$ . The spectral evolution of the SHG signal versus the delay between optical and THz pulses makes it possible to evidence the interference between volume and surface contributions as well as the ultrafast evolution of the hyper-Rayleigh susceptibility upon hot carrier generation.**

## I. INTRODUCTION

Lattice deformations resulting from the initial carrier distribution and lattice expansions caused by the excitation of a non-thermal phonon bath during carrier thermalization have been measured and predicted in silicon and other semiconductors [1]–[4]. Time resolved X-ray diffraction [2, 3] and electron diffraction [6], [7] experiments are nearly ideal tools to study lattice deformation induced by carrier relaxation. Hereafter, we demonstrate that recording the evolution of the spectrum of THz-induced SHG versus the delay between a sub-picosecond near infrared (IR) optical pulse and an ultrashort THz pulse makes it possible to follow the impact of the photo-carrier generation on the evolution of the IR active phonons in a (111) Si wafer with a sub-100 fs time resolution. This experiment also reveals the interference between the surface and bulk SHG.

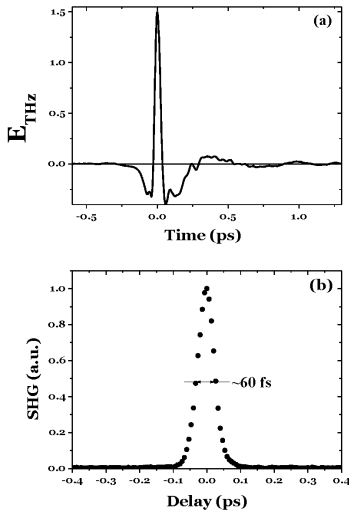


**Fig. 1.** a) Temporal evolution of the THz field. b) Temporal evolution of the THz-SHG signal reflected by a (111) silicon wafer and recorded with a photomultiplier.

## I. EXPERIMENTAL SETUP

The experiment is performed using a Ti:Sapphire

regenerative amplifier that yields at a 1 kHz repetition rate, 50 fs, 3.5 mJ pulses centered around 800 nm. A 1 mJ pulse is used to generate ultrashort THz pulse through a two-color plasma generation. The generated THz pulse is transmitted by a 1 mm thick silicon wafer, collimated and focused on the (111) silicon wafer by two off-axis parabolic mirrors. The temporal evolution of the ultrashort THz field is displayed in Fig. 1a. Our THz pulse is short ( $\sim 60$  fs) and its spectrum, centered about 5 THz, extends up to 45 THz. On the silicon wafer, set at an angle of incidence of  $45^\circ$ , the p-polarized THz pulse is mixed colinearly with a  $2 \mu\text{J}$  s-polarized near IR femtosecond pulse centered at  $\sim 800$  nm that pulse duration is  $\sim 50$  fs at full width at half maximum (FWHM). The near IR optical pulse, passing through the focusing off-axis parabolic mirror, is focused of silicon by a lens which focal length  $f=125$  cm. A delay line makes it possible to delay the near IR optical pulse with respect to the THz pulse. The reflected SHG signal generated on the silicon wafer is detected by a photomultiplier set at the exit of a monochromator. The THz pulse is chopped at 500 Hz and the SHG signal is recorded by a lock-in amplifier on which the photomultiplier is connected. The evolution of the THz induced SHG signal recorded when delaying the THz pulse is displayed in Fig. 1b. Its full width at half maximum is  $\sim 60$  fs, close to the FWHM of the near THz pulse.

The SHG spectrum is also recorded by a thermally cooled CCD camera installed at the exit of a spectrometer. It writes:  $E_{\text{SHG}} \sim \epsilon_0 [\chi^{(2)}(\omega, \omega, 2\omega) E^2(\omega) + \chi^{(3)}(\omega, \omega, \Omega, 2\omega \pm \Omega) E(\Omega) E^2(\omega)]$  where  $E(\omega)$ ,  $E(\Omega)$ ,  $\chi^{(2)}(\omega, \omega, 2\omega)$  and  $\chi^{(3)}(\omega, \omega, \Omega, 2\omega \pm \Omega)$  are the electric field of optical and THz pulses and the second- and third-order susceptibility of the studied material, respectively. Silicon being centrosymmetric,  $\chi^{(2)}(\omega, \omega, 2\omega)$  is the surface susceptibility. The SHG field at  $2\omega \pm \Omega$  appears when THz and optical pulses interact at the silicon surface. It results from a hyper-Raman scattering process.

## II. RESULTS

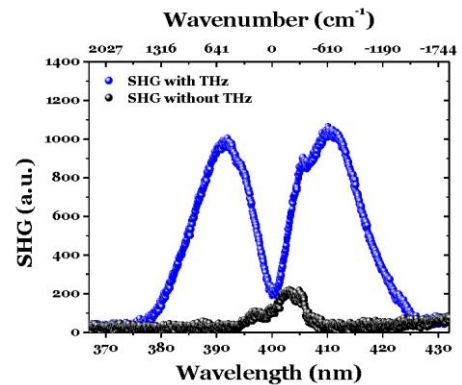


**Fig. 2.** SHG spectra with and without the THz pulse.

The SHG spectra recorded with and without the THz pulse

are displayed in Fig. 2. Without the THz pulse, the SHG signal is solely generated at silicon surface. It is centered at  $\lambda \sim 400$  nm. When THz pulse is applied and overlaps the optical pulse at zero-time delay, the SHG spectra displays a Stokes and anti-Stokes broadband shifted by about  $620 \text{ cm}^{-1}$ . The latter shift is associated to the enhancement of the  $\chi^{(3)}(\omega, \omega, \Omega, 2\omega \pm \Omega)$  centered around the Si lattice phonon wavenumber [8].

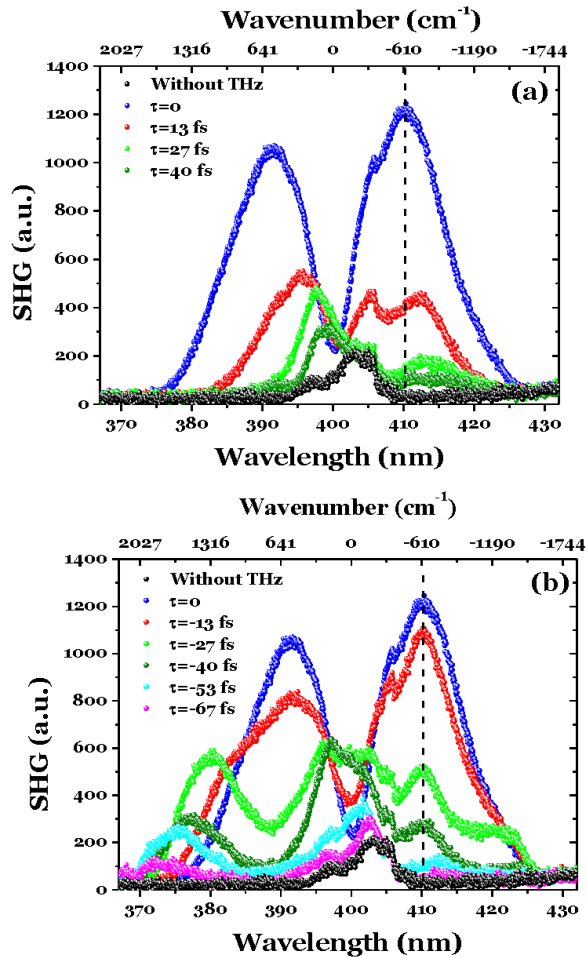


**Fig. 3.** Evolution of the SHG spectra versus the delay between the optical and THz pulses. The THz pulse hits the sample prior (a) or after (b) the optical pulse.

Afterward, the optical and THz pulses were delayed in time. The recorded spectra are displayed in Fig. 3. In agreement with Fig. 1b, the SHG signal rapidly decreases versus the delay between the optical and THz pulses. Besides, given a delay, the Stokes and anti-Stokes bands are broadened and their amplitude is higher when the optical pulse reaches the sample prior to the THz. This seems to indicate that the photo-carriers generated by the optical pump pulse modify the resonant contributions of  $\chi^{(3)}(\omega, \omega, \Omega, 2\omega \pm \Omega)$  within 100 fs time-scale. Finally, Fig. 3b also reveals the occurrence of modulations of the SHG spectra when the optical and THz pulse are delayed. The latter phenomena can be understood considering that the surface SHG and THz induced SHG spectral components can interfere giving rise to these spectral modulations [9]. We will show the spectral modulation depends on the delay between the optical and THz pulses and is more easily evidenced when the surface and THz

induced SHG have about the same amplitude, condition which can be fulfilled for a given range delay between the optical and THz pulses.

### III. SUMMARY

In summary, we performed a time-resolved THz induced SHG spectroscopy of a (111) silicon wafer, a technic which makes it possible to evidence the evolution of the hyper-Rayleigh susceptibility on the 100 fs time scale as well as the spectral interferences between the surface and bulk-THz induced SHG contributions.

### IV. REFERENCES

- [1] C. V. Shank, R. Yen, et C. Hirlimann, « Time-Resolved Reflectivity Measurements of Femtosecond-Optical-Pulse-Induced Phase Transitions in Silicon », *Phys. Rev. Lett.*, vol. 50, n° 6, p. 454-457, févr. 1983, doi: 10.1103/PhysRevLett.50.454.
- [2] A. M. Lindenberg *et al.*, « Atomic-Scale Visualization of Inertial Dynamics », *Science*, vol. 308, n° 5720, p. 392-395, avr. 2005, doi: 10.1126/science.1107996.
- [3] K. Sokolowski-Tinten *et al.*, « Femtosecond X-Ray Measurement of Ultrafast Melting and Large Acoustic Transients », *Phys. Rev. Lett.*, vol. 87, n° 22, p. 225701, nov. 2001, doi: 10.1103/PhysRevLett.87.225701.
- [4] M. Harb *et al.*, « Electronically Driven Structure Changes of Si Captured by Femtosecond Electron Diffraction », *Phys. Rev. Lett.*, vol. 100, n° 15, p. 155504, avr. 2008, doi: 10.1103/PhysRevLett.100.155504.
- [5] A. Rousse *et al.*, « Non-thermal melting in semiconductors measured at femtosecond resolution », *Nature*, vol. 410, n° 6824, p. 65-68, mars 2001, doi: 10.1038/35065045.
- [6] B. J. Siwick, J. R. Dwyer, R. E. Jordan, et R. J. D. Miller, « An Atomic-Level View of Melting Using Femtosecond Electron Diffraction », *Science*, vol. 302, n° 5649, p. 1382-1385, nov. 2003, doi: 10.1126/science.1090052.
- [7] C.-Y. Ruan, V. A. Lobastov, F. Vigliotti, S. Chen, et A. H. Zewail, « Ultrafast Electron Crystallography of Interfacial Water », *Science*, vol. 304, n° 5667, p. 80-84, avr. 2004, doi: 10.1126/science.1094818.
- [8] S. Hava, J. Ivri, et M. Auslender, « Wavenumber-modulated patterns of transmission through one- and two-dimensional gratings on a silicon substrate », *J. Opt. Pure Appl. Opt.*, vol. 3, n° 6, p. S190-S195, nov. 2001, doi: 10.1088/1464-4258/3/6/370.
- [9] F. Chen *et al.*, « Ultrafast Terahertz Gating of the Polarization and Giant Nonlinear Optical Response in BiFeO<sub>3</sub> Thin Films », *Adv. Mater.*, vol. 27, n° 41, p. 6371-6375, nov. 2015, doi: 10.1002/adma.201502975.